International Journal of Heat and Mass Transfer 52 (2009) 4675–4682

Contents lists available at ScienceDirect

International Journal of Heat and Mass Transfer

journal homepage: www.elsevier.com/locate/ijhmt

Experimental determination of thermal conductivity of three nanofluids and development of new correlations

Ravikanth S. Vajjha, Debendra K. Das *

Department of Mechanical Engineering, University of Alaska Fairbanks, P.O. Box 755905, Fairbanks, AK 99775-5905, USA

ARTICLE INFO

Article history:
Received 8 July 2008
Received in revised form 17 June 2009
Accepted 17 June 2009
Available online 25 July 2009

Keywords:
Nanofluids
Thermal conductivity
Ethylene glycol
Concentration
Temperature dependency

ABSTRACT

Experimental investigations have been carried out for determining the thermal conductivity of three nanofluids containing aluminum oxide, copper oxide and zinc oxide nanoparticles dispersed in a base fluid of 60:40 (by mass) ethylene glycol and water mixture. Particle volumetric concentration tested was up to 10% and the temperature range of the experiments was from 298 to 363 K. The results show an increase in the thermal conductivity of nanofluids compared to the base fluids with an increasing volumetric concentration of nanoparticles. The thermal conductivity also increases substantially with an increase in temperature. Several existing models for thermal conductivity were compared with the experimental data obtained from these nanofluids, and they do not exhibit good agreement. Therefore, a model was developed, which is a refinement of an existing model, which incorporates the classical Maxwell model and the Brownian motion effect to account for the thermal conductivity of nanofluids as a function of temperature, particle volumetric concentration, the properties of nanoparticles, and the base fluid, which agrees well with the experimental data.

1. Introduction

Nanofluids are the suspensions of nanometer-sized (<100 nm) solid particles in base fluids such as water, ethylene glycol or oil. In the last few years, nanofluids have gained significant attention due to their enhanced thermal characteristic. According to Eastman et al. [1], the effective thermal conductivity of ethylene glycol is increased by up to 40% when a 0.3 volumetric percent of copper nanoparticles of mean diameter less than 10 nm are dispersed in it. From heat transfer theory, for a constant Nusselt number, the convective heat transfer coefficient is directly proportional to the thermal conductivity. With this observation, many researchers have been motivated to determine the thermal conductivity of nanofluids accurately.

Lee et al. [2] measured thermal conductivity of Al_2O_3 and CuO nanoparticles in water and ethylene glycol via a transient hot-wire apparatus and concluded that thermal conductivity can be enhanced by more than 20% at a particle volumetric concentration of 4% for CuO/ethylene glycol mixture. Das et al. [3] presented experimental data on the temperature dependence of thermal conductivity of Al_2O_3 and CuO particles in water up to a volumetric concentration of 4% and within the temperature range of 21–51 °C. Their experimental data showed that for 1% particle volumetric concentration of CuO/water nanofluids, the thermal conductivity ratio increased from 6.5% to 29% over a temperature range of 21–51 °C. Yu and Choi [4] proposed a renovated Maxwell model including the effect of a nanolayer surrounding nanoparticles. They found that this nanolayer has a major impact on the effective thermal conductivity of nanofluids, for the particle diameter of less than 10 nm. Wang et al. [5] described a fractal model considering the surface adsorption of nanoparticles and showed a favorable comparison with their experiment for 50 nm CuO/deionized water of dilute concentration (<0.5%). Koo and Kleinstreuer [6,7] presented a thermal conductivity model for nanofluids which comprised of a static part and a dynamic part due to the Brownian movement of nanoparticles. Murshed et al. [8] measured the thermal conductivity of water-based TiO_2-nanofluid by the transient hot-wire method. Their results showed that the Hamilton and Crosser [9] model and the Bruggemen [10] model differed from their experimental data by about 17% for a 5% particle volumetric concentration. Xue and Xu [11] developed a model for thermal conductivity of nanofluids considering the effective thermal conductivity of an interfacial shell between the particle and the fluid. Chon et al. [12] presented an empirical correlation for Al_2O_3 nanofluid in water, based upon the Buckingham-Pi theorem; as a function of Prandtl number, particle Reynolds number based on the Brownian velocity, thermal conductivity of the particle and base fluid, volume fraction and particle size. Liu et al. [13] described a chemical reduction method for synthesizing copper nanofluid and showed thermal conductivity enhancement of 23.8% for 0.1%

* Corresponding author. Tel.: +1 907 474 6094; fax: +1 907 474 6141.
E-mail address: ffdkd@uaf.edu (D.K. Das).

0017-9310/$ - see front matter © 2009 Elsevier Ltd. All rights reserved.
doi:10.1016/j.ijheatmasstransfer.2009.06.027

Nomenclature

C_p	specific heat, J/kg K
d_p	particle diameter, m
k	thermal conductivity, W/m K
T	temperature, K
T_0	reference temperature, 273 K

Greek letters

β	fraction of liquid volume traveling with a particle
μ	coefficient of dynamic viscosity of the fluid, kg/m s
ϕ	particle volumetric concentration
ρ	density of the fluid, kg/m^3
κ	Boltzmann constant, 1.381×10^{-23} J/K

Subscripts

bf	base fluid
nf	nanofluid
p	particle

volumetric concentration of copper particles in water. Prasher et al. [14] also presented a Brownian motion based convective–conductive model for thermal conductivity of nanofluids. Jang and Choi [15] developed a model for nanofluid thermal conductivity that took into account the collision between base fluid molecules, thermal diffusion of nanoparticles in fluids, collision between nanoparticles and nano-convection due to Brownian motion. Li et al. [16] presented experimental data on Al_2O_3/water nanofluid of concentration up to 6% and temperature up to 37 °C by transient hot-wire method as well as a steady-state method. They observed that at room temperature both transient and the steady-state methods yield nearly identical values of the thermal conductivity of nanofluids, while at higher temperatures the onset of natural convection resulted in larger conductivity for the transient method than those obtained using steady-state method A comprehensive review of experimental and theoretical investigations on the thermal conductivity of nanofluids by various researchers was compiled by Wang and Mujumdar [17].

In cold regions of the world, such as Alaska, Canada, Northern Europe and Russia, it is a common practice to use 60% ethylene glycol and 40% water by mass (60:40 EG/W) as a heat transfer fluid in building heating systems, automobiles and heat exchangers (ASHRAE, [18]). At present no data exists for thermal conductivity of nanoparticles dispersed in 60:40 EG/W mixture, although it is the most widely used fluid for cold regions. All data available at present are for pure water, glycol or oil as base fluids. For this reason, in the present experiments, 60:40 EG/W is used as the base fluid in which nanoparticles are dispersed. This paper provides a comprehensive set of carefully measured thermal conductivity data for three nanofluids: aluminum oxide (Al_2O_3), copper oxide (CuO) and zinc oxide (ZnO) all dispersed in the base fluid 60:40 EG/W. Furthermore, in this study new correlations have been developed from the thermal conductivity data of three nanofluids for application over a wide range of temperatures and particle volumetric concentrations. These correlations have been tested for base fluids, water and 60:40 EG/W and show good agreement. Therefore, they can be used to determine accurately the thermal conductivity of nanofluids for different concentrations, different temperatures and different base fluids. For analytical and computational heat transfer studies, a relationship for thermal conductivity is necessary as input. The new correlations developed in this paper can fulfill those needs to evaluate the convective heat transfer coefficient of nanofluids.

The characteristics of nanofluids whose thermal conductivities were measured are summarized in Table 1. These nanofluids were procured from Alfa Aesar [19], as 50% dispersion in water. Subsequent particle volumetric concentrations were prepared by adding different proportions of 60:40 EG/W mixture to the manufacturer's fluid. Each nanofluid sample was agitated in an ultrasonicator for about 2 h before the experiments to ensure uniform particle dispersion. The temperature range (298–363 K) of experiments was selected to match the range at which building heating fluids, automobile coolants and many industrial heat exchangers operate in cold regions.

2. Existing theoretical and empirical equations

Starting from Maxwell [22], numerous experimental and theoretical studies have been conducted to predict the effective thermal conductivity of solid particles suspended in base fluids. The Maxwell model for effective thermal conductivity of solid–liquid mixtures is given for micro or millimeter sized particles suspended in base fluids.

$$k_{eff} = \frac{k_p + 2k_{bf} + 2(k_p - k_{bf})\phi}{k_p + 2k_{bf} - (k_p - k_{bf})\phi} k_{bf} \tag{1}$$

where k_{eff} is the thermal conductivities of the solid–liquid mixture. Maxwell's model is good for spherical shaped particles with low particle volume concentrations.

Bruggemen [10] proposed an implicit model for the effective thermal conductivity of solid–liquid mixtures, taking into account the interactions among the randomly distributed particles which is given as

$$\phi\left(\frac{k_p - k_{eff}}{k_p + 2k_{eff}}\right) + (1-\phi)\left(\frac{k_{bf} - k_{eff}}{k_{bf} + 2k_{neff}}\right) = 0 \tag{2}$$

Bruggemen's model can be applied to spherical particles with no limitations on the particle volumetric concentrations.

Hamilton and Crosser [9] extended the Maxwell's model by introducing a shape factor to account for the effect of the shape of particles. The effective thermal conductivity of the solid/liquid mixture is given as

$$k_{eff} = \frac{k_p + (n-1)k_{bf} - (n-1)\phi(k_{bf} - k_p)}{k_p + (n-1)k_{bf} + \phi(k_{bf} - k_p)} k_{bf} \tag{3}$$

where n is the empirical shape factor given by $3/\psi$, and ψ is the particle sphericity, defined as surface area of a sphere (with the same volume as the given particle) to the surface area of the particle. For spherical particle the value of n is 3.

However, all the above models were developed to predict the thermal conductivity of micro/millimeter sized particles suspended in base fluids. As these theories fail to predict the thermal conductivity of nanofluids, many new theories have been proposed in recent years. Based on the effective medium theory, Yu and Choi [4] proposed a modified Maxwell model to include the effect of a nanolayer surrounding the particles by replacing the thermal conductivity of solid particles with the equivalent thermal conductivity of particles k_{pe} which is given as

$$k_{pe} = \frac{[2(1-\gamma) + (1+\chi)^3(1+2\gamma)]\gamma}{-(1-\gamma) + (1+\chi)^3(1+2\gamma)} k_p \tag{4a}$$

where $\gamma = k_{layer}/k_p$ is the ratio of nanolayer thermal conductivity to particle thermal conductivity and $\chi = h/r$ is the ratio of the nanolayer

Table 1
Characteristics of nanofluids used in this study.

Type of nanoparticle	Density (kg/m^3)	Thermal conductivity (W/m K)	Particle size (nm)	Base fluid
Al_2O_3	3600 [19]	36 [20]	53	60:40 EG/W
ZnO	5600 [19]	13 [21]	29 and 77	60:40 EG/W
CuO	6500 [19]	17.65 [21]	29	60:40 EG/W and water

thickness to the particle radius. In their study, the nanolayer thickness h and the thermal conductivity k_{layer} are given to range from 1 to 2 nm and $10k_{bf} < k_{layer} < 100k_{bf}$, respectively. Finally the thermal conductivity of the nanofluid is given as

$$k_{nf} = \frac{k_{pe} + 2k_{bf} + 2(k_{pe} - k_{bf})(1+\chi)^3\phi}{k_{pe} + 2k_{bf} - (k_{pe} - k_{bf})(1+\chi)^3\phi}k_{bf} \tag{4b}$$

Xuan et al. [23] proposed a model considering the Brownian motion of nanoparticles and their aggregation. The modified correlation for the apparent thermal conductivity of nanofluid is the sum of the Maxwell's model and the term due to Brownian motion of the nanoparticles and clusters.

$$k_{nf} = \frac{k_p + 2k_{bf} - 2(k_{bf} - k_p)\phi}{k_p + 2k_{bf} + (k_{bf} - k_p)\phi}k_{bf} + \frac{\rho_p\phi C_{p_p}}{2}\sqrt{\frac{\kappa T}{3\pi\mu_{bf}r_c}} \tag{5}$$

Here r_c is the mean radius of gyration of the cluster and μ_{nf} is the viscosity of basefluid. Upon inspection, it is found that the second term of Eq. (5) does not yield the unit of the thermal conductivity (W/m K). Therefore, the equation is not dimensionally homogeneous. In order to satisfy the dimensional homogeneity, the constant coefficient $(\frac{1}{2\sqrt{3\pi}})$ should have a unit instead of being dimensionless. The only condition under which the Eq. (5) is dimensionally correct is by assigning a unit of $(m/\sqrt{s})$ to this constant coefficient, so that the whole term matches the unit of thermal conductivity.

Koo and Kleinstreuer [6,7] presented a thermal conductivity model which has a similar two-term function presented by Xuan et al. [23]. It takes into account the effect of particle size, particle volumetric concentration, temperature and properties of base fluid as well as nanoparticles subjected to Brownian motion. When compared with experimental data, this model predicts better than other models as shown in Fig. 9 presented in Section 4. According to their model the effective thermal conductivity of nanofluid is given as

$$k_{nf} = \frac{k_p + 2k_{bf} - 2(k_{bf} - k_p)\phi}{k_p + 2k_{bf} + (k_{bf} - k_p)\phi}k_{bf} + 5\times10^4\beta\phi\rho_{bf}C_{pbf} \times\sqrt{\frac{\kappa T}{\rho_p d_p}}f(T,\phi,\text{etc.}) \tag{6a}$$

where β represents the fraction of the liquid volume which travels with a particle and decreases with the particle volumetric concentration because of the viscous effect of moving particles. Table 2 shows the function β obtained by them for different nanoparticles as a function of particle volume concentration. Since from the kinetic theory, the dependence of thermal conductivity on temperature is weak, they introduced an empirical function $f(T,\phi)$ using the experimental data of Das et al. [3] on CuO nanofluids.

Table 2
Curve-fit relations proposed by Koo and Kleinstreuer [6].

Type of particles	β	Concentration
Au-citrate, Ag-citrate and CuO	$0.0137(100\phi)^{-0.8229}$	$\phi < 1\%$
CuO	$0.0011(100\phi)^{-0.7272}$	$\phi > 1\%$
Al_2O_3	$0.0017(100\phi)^{-0.0841}$	$\phi > 1\%$

$$f(T,\phi) = (-6.04\phi + 0.4705)T + (1722.3\phi - 134.63) \tag{6b}$$

They recommended the above equation in the ranges $1\% < \phi < 4\%$ and $300 < T < 325$ K. The first part of the Eq. (6a) is the particles' conventional static conductivity obtained directly from the Maxwell model while the second part accounts for the Brownian motion.

Xue and Xu [11] developed an implicit relation for the effective thermal conductivity of copper oxide/water and copper oxide/EG nanofluids based on a model of nanoparticles with interfacial shells between the surface of the solid particle and the surrounding liquid.

$$\left(1 - \frac{\phi}{\omega}\right) \times\frac{k_{nf} - k_{bf}}{2k_{nf} + k_{bf}} + \frac{\phi}{\omega}\frac{(k_{nf} - k_2)(2k_2 + k_p) - \omega(k_p - k_2)(2k_2 + k_{nf})}{(2k_{nf} + k_2)(2k_2 + k_p) + 2\omega(k_p - k_2)(k_2 - k_{nf})} = 0 \tag{7a}$$

$$\text{where}\quad \omega = \left[\frac{r_p}{r_p + t}\right]^3 \tag{7b}$$

In the above equation k_2 is the thermal conductivity of the interfacial shell and t represents the thickness of the interfacial shell, which are different for different nanofluids. The radius of the nanoparticle is r_p.

Chon et al. [12] proposed an empirical correlation for the thermal conductivity of Al_2O_3 nanofluid from their experimental data using Buckingham-Pi theorem with a linear regression scheme. They concluded that the Brownian motion of the suspended nanoparticle is the most important factor in the enhancement of thermal conductivity of nanofluids. The correlation is given as

$$\frac{k_{nf}}{k_{bf}} = 1 + 64.7\phi^{0.7460}\left(\frac{d_{bf}}{d_p}\right)^{0.3690}\left(\frac{k_p}{k_{bf}}\right)^{0.7476}\text{Pr}^{0.9955}\text{Re}^{1.2321} \tag{8}$$

where d_{bf} is the molecular diameter of the base fluid; $\text{Pr} = \frac{C_{pbf}\mu_{bf}}{k_{bf}}$ is the Prandtl number of the base fluid and $Re = \frac{(\rho_{bf}\kappa T)}{(3\pi\mu_{bf}^2 l_{bf})}$ is the Reynolds number; l_{bf} is the mean-free path for the base fluid. A constant value of 0.17 nm for the mean-free path l_{bf} was used in their paper for water for the entire tested temperature range.

Prasher et al. [14] proposed that the enhancement in the thermal conductivity of nanofluids is primarily due to the convection caused by the Brownian motion of the nanoparticles. They introduced a convective–conductive model, which is a combination of Maxwell–Garnett conduction model and the convection caused by the Brownian motion of suspended nanoparticles.

$$\frac{k_{nf}}{k_{bf}} = \left(1 + A\text{Re}^m\text{Pr}^{0.333}\phi\right)\left(\frac{[k_p(1+2\alpha) + 2k_m] + 2\phi[k_p(1-\alpha) - k_m]}{[k_p(1+2\alpha) + 2k_m] - \phi[k_p(1-\alpha) - k_m]}\right) \tag{9}$$

where the coefficient $A = 4\times10^4$; $m = 2.5 \pm (15\%\text{ of }2.5)$ for water-based nanofluids, $m = 1.6 \pm (15\%\text{ of }1.6)$ for EG-based nanofluids and $m = 1.05 \pm (15\%\text{ of }1.05)$ for oil-based nanofluids; $k_m = k_{bf}[1 + (1/4)\text{Re}\cdot\text{Pr}]$ is the matrix conductivity; $\text{Re} = \frac{1}{\nu}\sqrt{\frac{18\kappa T}{\pi\rho_p d_p}}$ is the Brownian–Reynolds number; $\alpha = 2R_b k_m/d_p$ is the nanoparticle

Biot number; R_b is the interfacial thermal resistance between nanoparticles and different fluids; v is the kinematic viscosity and Pr is the Prandtl number of the base fluid.

Jang and Choi [15] proposed a theoretical model that involves four modes contributing to the energy transfer resulting in enhancement of thermal conductivity of nanofluids. The first mode is collision between base fluid molecules, the second mode is the thermal diffusion in nanoparticles, the third mode is the collision of nanoparticles with each other due to the Brownian motion, and the fourth mode is collision between base fluid molecules and nanoparticles by thermally induced fluctuations. Including all the above four modes, the effective thermal conductivity of nanofluid is given as

$$k_{nf} = k_{bf}(1-\phi) + \beta_1 k_p \phi + C_1 \frac{d_{bf}}{d_p} k_{bf} \mathrm{Re}_{d_p}^2 \mathrm{Pr} \phi \tag{10}$$

where $\beta_1 = 0.01$ is a constant for considering the Kapitza resistance per unit area; $C_1 = 18 \times 10^6$ is a proportionality constant; Pr is the Prandtl number of the base fluid, and the Reynolds number is defined by $\mathrm{Re}_{d_p} = \frac{\overline{C}_{R.M.} d_p}{v}$ where $\overline{C}_{R.M.} = \frac{\kappa T}{3\pi \mu_{bf} d_p l_{bf}}$ is the random motion velocity of a nanoparticle and v is the kinematic viscosity of base fluid. They recommend, for water-based nanofluids the equivalent diameter $d_{bf} = 0.384$ nm and mean-free path $l_{bf} = 0.738$ nm at a temperature of 300 K.

Vajjha and Das [24] measured thermal conductivity of Al_2O_3 nanofluid and showed its variation with particle volumetric concentration and temperature. Following the polynomial approach of Yaws [25] that has been successfully applied to many industrially important compounds, they proposed an empirical model which included the dependence of temperature and concentration in the following form.

$$k_{nf}(\phi, T) = A(\phi) + B(\phi)T + C(\phi)T^2 \tag{11}$$

The coefficients A, B, C are polynomial functions of concentration ϕ and are listed in [24].

3. Experimental setup and procedure

The apparatus constructed by Hilton [26] for thermal conductivity measurements of liquids and gases has been used in this study for the nanofluids. A schematic diagram of the experimental setup is shown in Fig. 1. The apparatus consists of a cylindrical water jacket surrounding an aluminum cylindrical plug, which houses a cartridge heater. The fluid whose thermal conductivity is to be measured is injected into the small radial clearance Δr between the heated plug and the water cooled jacket. The radial clearance has been designed to be very small ($\Delta r = 0.3$ mm) so that natural convection in the fluid lamina is prevented. The power input to the cartridge heater heating the aluminum plug is measured with precision through the voltmeter and ammeter of the heat transfer service unit shown in Fig. 1. The aluminum plug is designed to possess low thermal inertia and a minimal temperature variation along its length.

The plug is held centrally in the water jacket by 'O' rings that seal the radial clearance holding the fluid. Precision thermocouples are placed close to the external surface of the plug and the internal surface of the cooling jacket. Due to the positioning of the thermocouples and the high thermal conductivity of the materials involved, the temperatures measured are effectively the temperatures of the hot and cold faces of the fluid lamina. As recommended by the manufacturer of the apparatus, a calibration curve is prepared using air as the test fluid, whose thermal conductivity is accurately known to represents the incidental heat transfer $\dot{Q}_i$ versus the temperature difference ΔT of the hot and cold surfaces. This incidental heat transfer includes all heat transfer from the element in plug other than that transferred by the conduction through the fluid. Temperatures are measured by the heat transfer service unit and a data logger for comparison. Heater voltage and current are increased in steps and temperatures are measured when they reach steady state for each power input. Unlike the transient hot-wire method, the present procedure is a steady-state method for determining the thermal conductivity of fluids.

Electrical power input $\dot{Q}_e$ is measured by the standard panel mounted voltmeter and ammeter of the heat transfer service unit and they can be controlled using the panel mounted control knob. The conduction heat transfer rate $\dot{Q}_c$ is obtained by taking the difference between the electrical power input and the incidental heat transfer rate $\dot{Q}_i$ from the calibration curve. The thermal conductivity of nanofluid is obtained from the following equation

$$k_{nf} = \frac{\dot{Q}_c \Delta r}{A(\Delta T)} \tag{12}$$

In the above equation A is the effective area of conducting path through the fluid provided by the manufacturer.

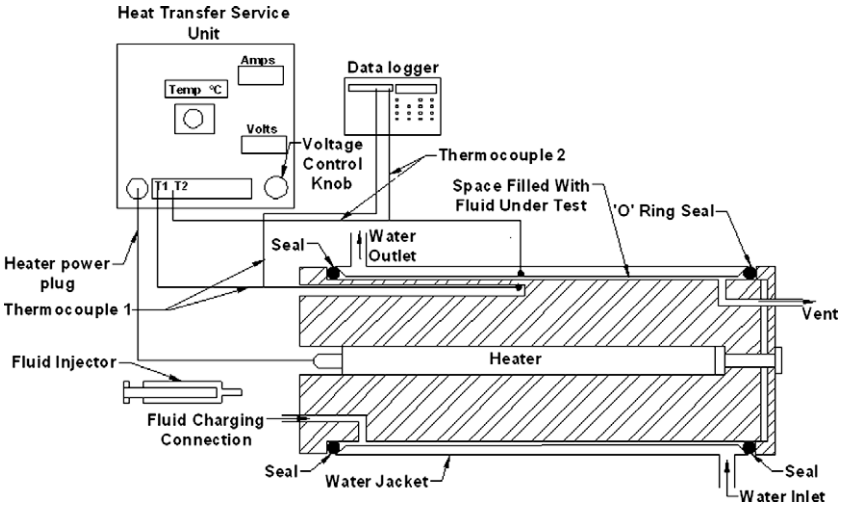

Fig. 1. Thermal conductivity measuring apparatus.

3.1. Uncertainty of experimental data

The uncertainty of thermal conductivity measurements was determined from the standard approach presented by Coleman and Steele [27].

$$\frac{\delta k}{k} = \left[\left(\frac{\delta \dot{Q}_e}{\dot{Q}_e}\right)^2 + \left(\frac{\delta \dot{Q}_i}{\dot{Q}_i}\right)^2 + \left(\frac{\delta(\Delta r)}{\Delta r}\right)^2 + \left(\frac{\delta A}{A}\right)^2 + \left(\frac{\delta(\Delta T)}{\Delta T}\right)^2\right]^{1/2} \tag{13a}$$

Heat conducted through the nanofluid $\dot{Q}_c = \dot{Q}_e - \dot{Q}_i$ and $\dot{Q}_e = VI$ where V is the voltage and I is the current applied to the cartridge heater. For the voltmeter and ammeter of modern design in the heat transfer service unit, the uncertainty in measurements $\frac{\delta V}{V}$ and $\frac{\delta I}{I}$ are about 0.5%. Therefore, the uncertainty in $\dot{Q}_e$ is

$$\frac{\delta \dot{Q}_e}{\dot{Q}_e} = \left[\left(\frac{\delta V}{V}\right)^2 + \left(\frac{\delta I}{I}\right)^2\right]^{1/2} \tag{13b}$$

Incidental heat transfer $\dot{Q}_i$ is obtained from the calibration curve which is a plot of $\dot{Q}_i$ versus temperature difference $(T_1 - T_2)$ between the plug temperature and jacket temperature, respectively.

$$\frac{\delta \dot{Q}_i}{\dot{Q}_i} = \left[\left(\frac{\delta T_1}{T_1}\right)^2 + \left(\frac{\delta T_2}{T_2}\right)^2\right]^{1/2} \tag{13c}$$

The uncertainty in measurements of temperature for type-K thermocouple [28] used in this apparatus is 0.6 °C between 0 and 100 °C. Therefore, at the mean temperature of 60 °C within the range of measurements, $(\frac{\delta T}{T}) = 1\%$.The uncertainty in length measurement $\frac{\delta r}{r}$ by the modern metrological gage is about 0.5%. The area A is proportional to the square of the linear dimension L, so the uncertainty in area measurement is $\frac{\delta A}{A} = [(2\frac{\delta L}{L})^2]^{1/2}$. The uncertainty in ΔT measurement is $\frac{\delta(\Delta T)}{\Delta T} = [(\frac{\delta T_1}{T_1})^2 + (\frac{\delta T_2}{T_2})^2]^{1/2}$. Finally combining all the above uncertainties together, the uncertainty in measurement of thermal conductivity is

$$\frac{\delta k}{k} = \left[\left(\frac{\delta V}{V}\right)^2 + \left(\frac{\delta I}{I}\right)^2 + \left(\frac{\delta T_1}{T_1}\right)^2 + \left(\frac{\delta T_2}{T_2}\right)^2 + \left(\frac{\delta r_1}{r_1}\right)^2 + \left(\frac{\delta r_2}{r_2}\right)^2 + \left(2\frac{\delta L}{L}\right)^2 + \left(\frac{\delta T_1}{T_1}\right)^2 + \left(\frac{\delta T_2}{T_2}\right)^2\right]^{1/2} = 2.45\%. \tag{13d}$$

3.2. Benchmark test cases

Before applying the apparatus and the experimental procedure to nanofluids, they were first tested with water and 60:40 EG/W whose thermal conductivities are accurately known. Fig. 2 shows the comparison between measured thermal conductivity and the values from Bejan [29] and ASHRAE [18] for water and 60:40 EG/W, respectively. A maximum deviation of 1.8% at 323 K for water and a maximum deviation of 1.7% at 298 K for 60:40 EG/W were observed when compared between measured values and the data from Bejan and ASHRAE, respectively. In the equations given if Fig. 2, the temperature is in Kelvin and the thermal conductivity is in W/m K. The base fluid thermal conductivity k_{bf} equation derived for 60:40 EG/W using ASHRAE data in Fig. 2 has been used in all subsequent calculations.

3.3. Al_2O_3 nanofluid

After qualifying the apparatus and the procedure with the benchmark test cases, the experimental setup was used for measuring the thermal conductivity of nanofluids. Fig. 3 presents a comparison between the experimental data and those predicted by Hamilton and Crosser [9] correlation for thermal conductivity of Al_2O_3 nanofluid of 6% particle volumetric concentration in a base fluid of 60:40 EG/W. The data shows that the thermal conductivity increases as the square of the temperature for this nanofluid within the range of temperature of the experiment. It is noticed that the Hamilton–Crosser correlation underpredicts the thermal conductivity values. The thermal conductivity k_{bf} of the base fluid (60:40 EG/W) from the ASHRAE curve-fit data is shown in Fig. 3 to illustrate the magnitude of conductivity enhancement by the nanoparticles over the base fluid. The percentage increase of thermal conductivity with temperature of the nanofluid predicted by Hamilton–Crosser's correlation is of the same magnitude as that of the base fluid, as both curves run nearly parallel. With increase in temperature the deviation between experimental data and the Hamilton–Crosser correlation increases.

The ratio of thermal conductivity of nanofluid to base fluid variation with temperature for volumetric concentrations ranging from 0% to 10% of Al_2O_3 nanofluid is displayed in Fig. 4. It is observed that the thermal conductivity ratio increases with an increase in temperature and also with an increase in particle volumetric concentration. As an example, for a 6% concentration, the thermal conductivity ratio increases from 1.224 to 1.478, a 21% increase between 298 and 363 K. For the 10% concentration

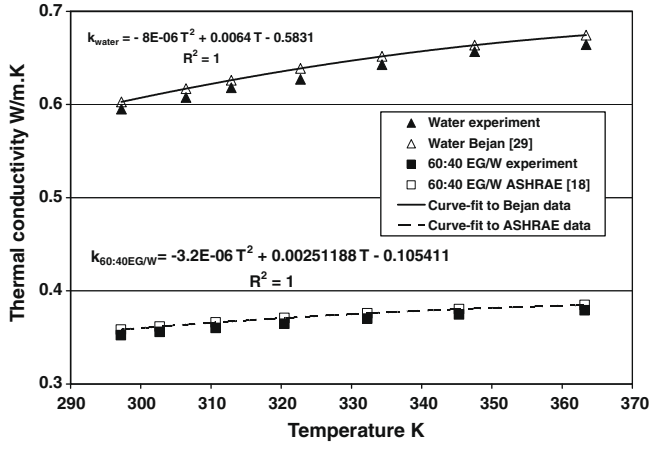

Fig. 2. Benchmark test cases for the thermal conductivity of water and 60:40 EG/W.

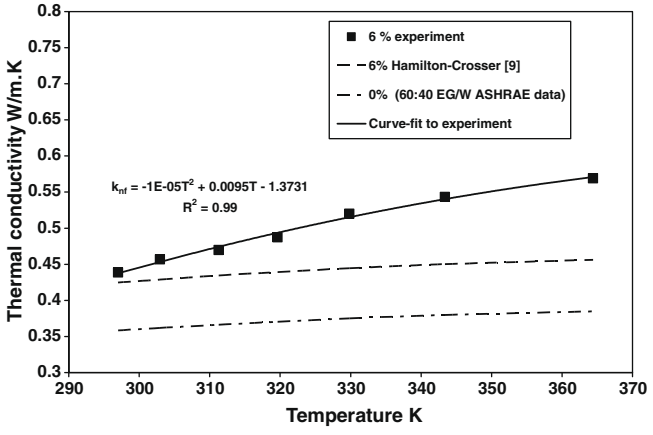

Fig. 3. Comparison of thermal conductivity variation with temperature between experimental values and Hamilton–Crosser correlation for a 6% Al_2O_3 nanofluid.

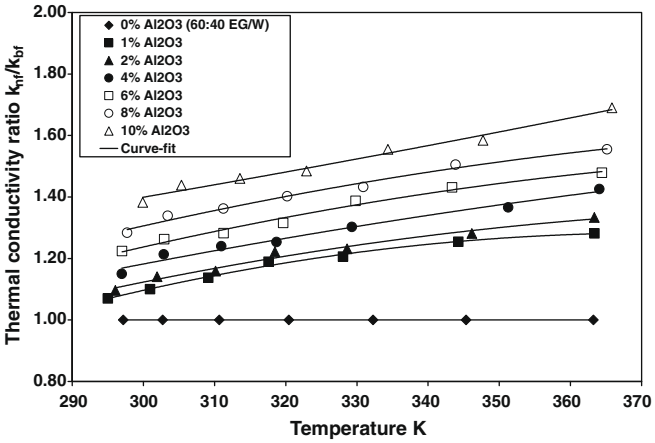

Fig. 4. Thermal conductivity ratio variation with temperature at different particle volumetric concentration of Al_2O_3 nanoparticles in 60:40 EG/W.

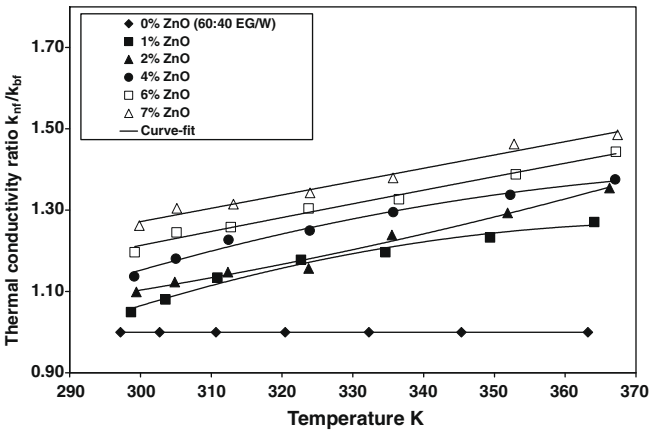

Fig. 6. Thermal conductivity ratio variation with temperature at different particle volumetric concentrations of ZnO nanoparticles in 60:40 EG/W.

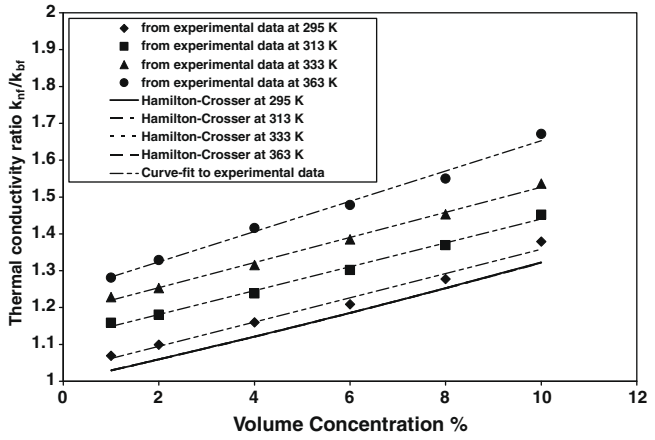

Fig. 5. Thermal conductivity ratio variation with volumetric concentration of Al_2O_3 nanoparticles in 60:40 EG/W with increase in temperature and comparison with Hamilton–Crosser correlation.

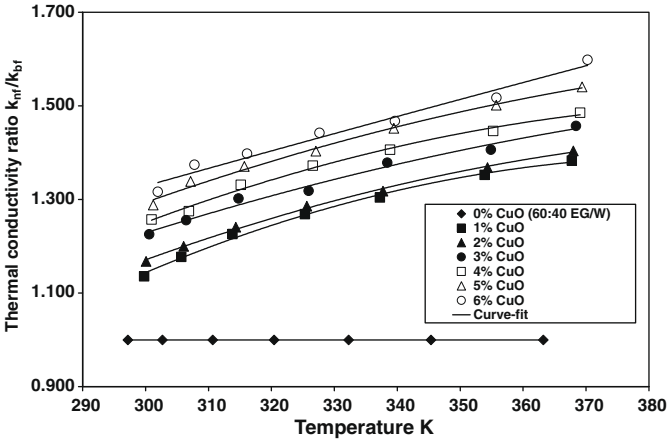

Fig. 7. Thermal conductivity ratio variation with temperature at different particle volumetric concentrations of CuO nanoparticles in 60:40 EG/W.

nanofluid at a temperature of 365 K, the thermal conductivity ratio increases over the base fluid by 69%.

After examining the temperature dependency of thermal conductivity, its dependence on particle concentration was examined. Fig. 5 shows the variation of thermal conductivity ratio of Al_2O_3 nanofluid as a function of the particle volumetric concentration. As observed, the thermal conductivity ratio increases with temperature as well as concentration. The Hamilton–Crosser correlation is unable to predict the correct thermal conductivity values. The values calculated from this correlation for four temperatures varying from 295 to 363 K overlap on one another to give a single curve in Fig. 5. Therefore, the Hamilton–Crosser correlation is not able to capture the influence of temperature. To asses the thermal conductivity ratio enhancement with concentration, we observe an increase by 29% from a concentration of 1% to 10% at a temperature of 295 K. From the nature of the curves, it is observed that for a constant temperature, the thermal conductivity ratio increases linearly with particle volumetric concentration.

3.4. ZnO nanofluid

Fig. 6 shows the variation of thermal conductivity ratio of ZnO nanofluid with temperature. As observed earlier, the thermal conductivity ratio increases with an increase in temperature as well as particle volumetric concentration. As an example, the increase in magnitude of thermal conductivity ratio for a 7% concentration is 18% between 298 and 363 K. For the same concentration nanofluid at a temperature of 363 K, the thermal conductivity ratio increases over the base fluid by 48.5%.

3.5. CuO nanofluid

Fig. 7 presents the thermal conductivity ratio versus the temperature for CuO nanofluid in a base fluid of 60:40 EG/W. Similar to observations made for the previous two nanofluids, the thermal conductivity ratio increases with an increase in temperature and concentration. To present a typical value of this enhancement, the thermal conductivity ratio for a 6% concentration increases by 21.4% between 298 and 363 K. For the same concentration CuO nanofluid at a temperature of 363 K, the thermal conductivity ratio increases over the base fluid by 60%.

3.6. Particle size effect

In order to assess the influence of nanoparticle size on the thermal conductivity, two sets of measurements were conducted with ZnO nanofluids of particle sizes 29 and 77 nm. The results are shown in Fig. 8 for thermal conductivity ratio as a function of temperature. From the figure it is observed that the thermal conductivity ratio is higher for smaller size nanoparticles. This behavior is intuitively correct as the thermal energy transfer is dependent on surface area and smaller particles of same volumetric concentration

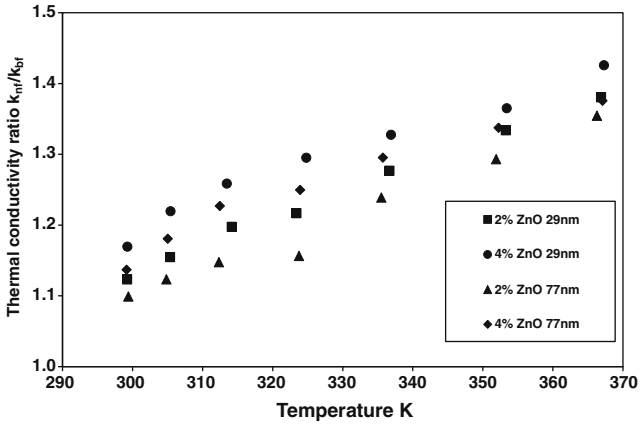

Fig. 8. Effect of nanoparticle size on nanofluid thermal conductivity ratio for varying temperatures at two different particle volumetric concentrations of ZnO nanofluid in 60:40 EG/W.

provide more surface area for the transfer of thermal energy. Therefore, the effective thermal conductivity is higher for smaller particles. This assertion is confirmed by the correlation, Eq. (14a) derived from the experimental data in the following section, which shows that the thermal conductivity of nanofluid is inversely proportional to the nanoparticle diameter. To get a sense of the order of magnitude increase, at 305 K the thermal conductivity ratio is 3% higher for 29 nm particle over that of 77 nm particle at a volumetric concentration of 2%. For the 4% volumetric concentration the thermal conductivity ratio is 3.3% higher for 29 nm particle over that of the 77 nm particle.

4. Development of new correlations

Our experimental results comprised of 133 data points derived from three different nanofluids. This data included the particle sizes of 29, 53 and 77 nm as listed in Table 1. We analyzed several existing thermal conductivity models and compared them against our experimental data. It was found that the correlation given by Koo and Kleinstreuer [6] matched the results better than the other existing models. However, the correlation of Koo and Kleinstreuer is based on a limited amount of data obtained from experiments on nanofluids over the temperature range 293 K < T < 325 K and concentration range 1% < ϕ < 4%. Therefore, we proceeded to improve this model by deriving new empirical correlations for β and $f(T,\phi)$ from our set of experimental data. The thermal conductivity model remains the same; however, new empirical correlations were derived from a broader set of data derived from three nanofluids.

$$k_{nf} = \frac{k_p + 2k_{bf} - 2(k_{bf} - k_p)\phi}{k_p + 2k_{bf} + (k_{bf} - k_p)\phi} k_{bf} + 5 \times 10^4 \beta \phi \rho_{bf} C_{pbf} \sqrt{\frac{\kappa T}{\rho_p d_p}} f(T,\phi) \tag{14a}$$

$$f(T,\phi) = (2.8217 \times 10^{-2}\phi + 3.917 \times 10^{-3})\left(\frac{T}{T_0}\right) + (-3.0669 \times 10^{-2}\phi - 3.91123 \times 10^{-3}) \tag{14b}$$

Table 3
Curve-fit relations for proposed from present experiments.

Type of particles	β	Concentration	Temperature
Al_2O_3	$8.4407(100\phi)^{-1.07304}$	$1\% \leqslant \phi \leqslant 10\%$	298 K $\leqslant T \leqslant$ 363 K
ZnO	$8.4407(100\phi)^{-1.07304}$	$1\% \leqslant \phi \leqslant 7\%$	298 K $\leqslant T \leqslant$ 363 K
CuO	$9.881(100\phi)^{-0.9446}$	$1\% \leqslant \phi \leqslant 6\%$	298 K $\leqslant T \leqslant$ 363 K

Notice that the β correlation came out to be the same for Al_2O_3 and ZnO, but differed slightly for CuO. However, the function $f(T, \phi)$ is same for all three nanofluids. The obtained correlations for Al_2O_3, ZnO and CuO are given in Table 3. The applicable range of particle size for using the above correlation is 29–77 nm.

4.1. Justification from experimental evidence

From experimental observation in Fig. 5 the thermal conductivity ratio appears to be a linear function of concentration ϕ. Since, Eq. (14a) is nearly a linear function of ϕ, there is an agreement with the experimental evidence and this model. From the experimental data in Fig. 3 we observed that thermal conductivity varies as the square of the temperature T for $R^2 = 0.99$. Considering Eq. ((14a) and (14b)) the exponent of T is 1.5, which is closer to the empirical evidence, rather than the weak dependence of $T^{0.5}$ predicted by the kinetic theory. Furthermore, from the observation on particle diameter effect presented in Fig. 8, there is an inverse relationship between k_{nf} and d_p which is supported by the Brownian motion theory.

To verify the validity of these new correlations, Eqs. ((14a) and (14b)), for a different base fluid, we applied it to water-based nanofluids. We conducted additional experiment with CuO nanoparticles in water as base fluid to compare the present correlation Eqs. ((14a) and (14b)) with the experimental data, as shown in Fig. 9. In this figure, the performances of various models are also shown. It is observed that Koo and Kleinstreuer model agrees with experimental data up to a temperature of 325 K for which it was developed. Beyond this range the correlation overpredicts the conductivity ratio. The models of Maxwell [22] and Yu and Choi [4] do not show any noticeable increase in thermal conductivity with temperature. For Yu and Choi correlation, h is taken to be 2 nm and k_{layer} is taken as $50k_{bf}$.The model of Jang and Choi [15] shows an extreme rise of thermal conductivity with temperature. The model of Chon et al. [12] underpredicts the value at lower temperatures. For the model of Prasher et al. [14], m is taken as 2.5% and $R_b = 0.77 \times 10^{-8}$ m^2 K/W for water-based nanofluids. This model underpredicts the thermal conductivity value at lower temperature and overpredicts at higher temperature.

Fig. 10 serves as a verification of the accuracy of the new correlation, Eqs. ((14a) and (14b)), in comparison with the Al_2O_3 thermal conductivity experimental data. The reason we have selected Al_2O_3 nanofluid is, it was measured up to the highest particle volumetric concentration of 10% among the three nanofluids. There is a good agreement between the experimental data and Eqs. ((14a)

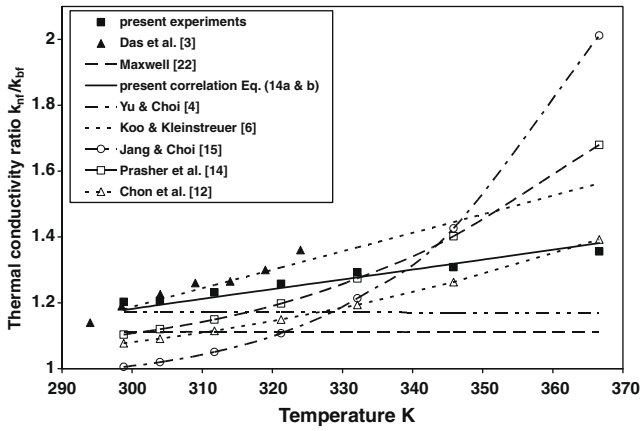

Fig. 9. Comparison between several theoretical models and experimental data on thermal conductivity for CuO/water nanofluids of 4% particle volumetric concentration.

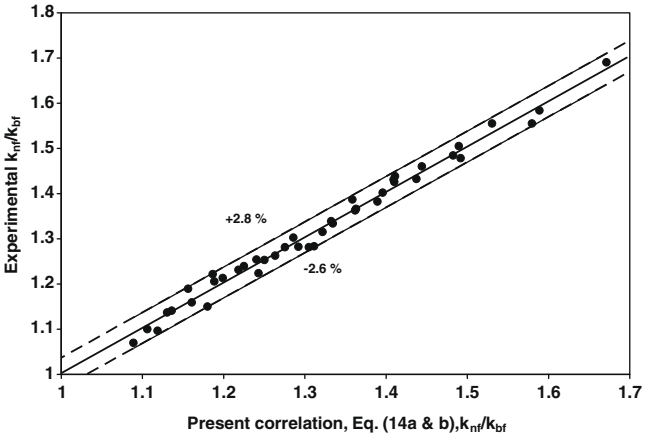

Fig. 10. Comparison of the thermal conductivity ratio calculated from the present correlation (Eq. (14a) and (14b)) with the values obtained from experiments on Al_2O_3 nanofluid.

and (14b)), with maximum deviations of +2.8%, −2.6% and the average deviation of 0.23% for Al_2O_3 nanofluid. For the ZnO nanofluid, the maximum deviations are +6.2%, −2.4% and the average deviation of 1.97%. For the CuO nanofluid, the maximum deviations are +7.7%, −0.0% and the average deviation of 5.74%.

5. Conclusions

From a set of carefully conducted experiments, the thermal conductivities of three nanofluids were measured over a temperature range of 298–363 K for various particle volumetric concentrations. The results showed an increase in thermal conductivity of nanofluid with increase in concentration and temperature. As the nanoparticle diameter increases, the thermal conductivity decreases. The correlation by Hamilton–Crosser does not capture the thermal conductivity variation with temperature. It is observed that many existing thermal conductivity models of nanofluids do not agree well with the present experimental results. The model by Koo and Kleinstreuer [6] has been improved by using a broader set of experimental data, which provided new correlations. These new correlations give accurate prediction of thermal conductivity of different nanofluids over a wide range of concentration and temperature. Since the nanofluids exhibit enhanced thermal conductivity with an increase in temperature, it is concluded that their application in higher temperature environment will be more beneficial.

Acknowledgements

Financial assistance from the Department of Mechanical Engineering and EPSCoR, Alaska at the University of Alaska Fairbanks is gratefully acknowledged.

References

[1] J.A. Eastman, S.U. S Choi, S. Li, W. Yu, L.J. Thompson, Anomalously increased effective thermal conductivities of ethylene glycol-based nanofluids containing copper nanoparticles, Appl. Phys. Lett. 78 (6) (2001) 718–720.
[2] S. Lee, S.U.S. Choi, S. Li, J. Eastman, Measuring thermal conductivity of fluids containing oxide nanoparticles, J. Heat Transfer 121 (1999) 280–289.
[3] S. Das, N. Putra, P. Thiesen, W. Roetzel, Temperature dependence of thermal conductivity enhancement for nanofluids, J. Heat Transfer 125 (2003) 567–574.
[4] W. Yu, S. Choi, The role of interfacial layers in the enhanced thermal conductivity of nanofluids: a renovated Maxwell model, J. Nanoparticle Res. 5 (2003) 167–171.
[5] B-X. Wang, L.-P. Zhou, X.-F. Peng, A fractal model for predicting the effective thermal conductivity of liquid suspension of nanoparticles, Int. J. Heat Mass Transfer 46 (2003) 2665–2672.
[6] J. Koo, C. Kleinstreuer, A new thermal conductivity model for nanofluids, J. Nanoparticle Res. 6 (2004) 577–588.
[7] J. Koo, C. Kleinstreuer, Laminar nanofluid flow in microheat-sinks, Int. J. Heat Mass Transfer 48 (2005) 2652–2661.
[8] S.M.S. Murshed, K.C. Leong, C. Yang, Enhanced thermal conductivity of TiO_2-water based nanofluids, Int. J. Thermal Sci. 44 (2005) 367–373.
[9] R. Hamilton, O. Crosser, Thermal conductivity of heterogeneous two-component systems, I and EC Fundamentals 125 (3) (1962) 187–191.
[10] D.A.G. Bruggemen, Berechnung Verschiedener Physikalischer Konstanten von Heterogenen Substanzen, I. Dielektrizitatskonstanten und Leitfahigkeiten der Mischkorper aus Isotropen Substanzen, Ann. Phys. Leipzig 24 (1935) 636–679.
[11] Q. Xue, W. Xu, A model of thermal conductivity of nanofluids with interfacial shells, Chem. Phys. 90 (2005) 298–301.
[12] C.H. Chon, K.D. Kihm, S.P. Lee, S.U.S. Choi, Empirical correlation finding the role of temperature and particle size for nanofluid (Al_2O_3) thermal conductivity enhancement, Appl. Phys. Lett. 87 (15) (2005) 153107.
[13] M.S. Liu, M.C.-C. Lin, C.Y. Tsai, C.-C. Wang, Enhancement of thermal conductivity with Cu for nanofluids using chemical reduction method, Int. J. Heat Mass Transfer 49 (2006) 3028–3033.
[14] R. Prasher, P. Bhattacharya, P.E. Phelan, Brownian-motion-based convective–conductive model for the effective thermal conductivity of nanofluids, J. Heat Transfer 128 (2006) 588–595.
[15] S.P. Jang, S.U.S. Choi, Effects of various parameters on nanofluid thermal conductivity, J. Heat Transfer 129 (2007) 617–623.
[16] C.H. Li, W. Williams, J. Buongiorno, L-W. Hu, G.P. Peterson, Transient and steady-state experimental comparison study of effective thermal conductivity of Al_2O_3/water nanofluids, J. Heat Transfer 130 (2008) 042407.
[17] X.-Q. Wang, A.S. Mujumdar, Heat transfer characteristics of nanofluids: a review, Int. J. Thermal Sci. 46 (2007) 1–19.
[18] ASHRAE Handbook, Fundamentals, American Society of Heating, Refrigerating and Air-Conditioning Engineers Inc., Atlanta, GA, 2005.
[19] Alfa Aesar. Available from: <http://www.alfaaesar.com/>, 2007.
[20] F.P. Incropera, D.P. DeWitt, Introduction to Heat Transfer, third ed., John Wiley & Sons, Inc., New York, 1996.
[21] R. Bolz, G. Tuve, Handbook of Tables for Applied Engineering Science, second ed., CRC Press, 2007.
[22] J.C. Maxwell, A Treatise on Electricity and Magnetism, second ed., Oxford University Press, Cambridge, UK, 1904.
[23] Y. Xuan, Q. Li, W. Hu, Aggregation structure and thermal conductivity of nanofluids, AIChE J. 49 (4) (2003) 1038–1043.
[24] R.S. Vajjha, D.K. Das, Measurement of thermal conductivity of Al_2O_3 nanofluid and development of a new correlation, in: T. Marbach (Ed.), Proceedings of 40th Heat Transfer and Fluid Mechanics Institute, Sacramento, CA, 2008, p.14.
[25] C.L. Yaws, Physical Properties – A Guide to the Physica Thermodynamic and Transport Property Data of Industrially Important Chemical Compounds, McGraw-Hill, New York, 1977.
[26] Experimental Operating and Maintenance Procedures for Thermal Conductivity of Liquids and Gases Unit, P.A. Hilton Ltd., Hampshire, England, 2005.
[27] H.W. Coleman, W.G. Steele, Experimentation and Uncertainty Analysis for Engineers, 2nd ed., John Wiley & Sons, Inc., New York, 1999.
[28] The Data Acquisition Systems Handbook, Omega Engineering Inc., Stamford, CT, 2005.
[29] A. Bejan, N. John, Heat Transfer, John Wiley & Sons, Inc., New York, 1993.